

## Competing fragment emissions in $^{12,13}\text{C} + ^{12}\text{C}$ reactions within collective clusterization mechanism

Rupinder Kaur<sup>1</sup>, Sarbjeet Kaur<sup>2</sup>, BirBikram Singh<sup>2,\*</sup>, B.S. Sandhu<sup>1</sup>, and S.K. Patra<sup>3</sup>

<sup>1</sup>Department of Physics, Punjabi University, Patiala-147002, India.

<sup>2</sup>Department of Physics, Sri Guru Granth Sahib World University, Fatehgarh Sahib-140406, India. and

<sup>3</sup>Institute Of Physics, Sachivalya Marg, Bhubhaneswar-751005, India

### Introduction

Nucleon clusterisation has been widely used to explain a number of nuclear phenomena within nuclear cluster models by treating the nucleons as a cluster rather than free nucleons. The well known examples of nuclear clustering is the tightly bound alpha particle and Hoyle state of  $^{12}\text{C}$ . Low-energy heavy ion collisions leading to the decay products of the very-light-mass composite systems ( $A = 20-40$ ) have been studied extensively, specifically for the composite systems in which neutron and proton numbers differs or are equal [1-4]. The clusterisation has been well explained within the Dynamical Cluster Decay model (DCM) [2-4] studies. These studies have revealed that, the minima in the potential-energy surface (PES) lie at  $\alpha$ -particle-like nuclei in case of  $N = Z$ , where as the minima start to appear at non- $\alpha$  clusters with the addition of the neutrons to either the projectile or target or both. A competition between various processes like FF and DIO and nuclear cluster structure has also shown to play significant role in some cases [2, 4].

It makes an interesting case to study few more composite nuclei in this mass region to develop a systematics. With this motivation, we intend to extend the study [3] by investigating fragments emission from composite nuclei (CN)  $^{24,25}\text{Mg}^*$  formed in the reactions  $^{12,13}\text{C} + ^{12}\text{C}$  at  $E_{lab} \sim 6$  MeV/nucleon [6], within DCM to give a dynamical description of the mechanism based on collective clusterization approach. The fragmentation po-

tential for both the CN  $^{24,25}\text{Mg}^*$  was presented and quite interestingly the results for the most favoured or minimized fragments are in line with the experimental findings which show the enhancement in the measured yields of fragments with respect to the specific exit channels containing the complementary binary fragment as  $\alpha$ -cluster or neighbouring nuclei. This preliminary study has been extended here further to calculate the fragment cross sections, which includes penetration of the preformed fragment through the scattering potential barrier, within the DCM, described briefly in the following sections. The calculations, discussions and results and, their comparison with the experimental data [6], is presented in the last section.

### Methodology

The Dynamical cluster decay model (DCM) [2-5] of Gupta and collaborators is worked out in terms of collective co-ordinates of mass (and charge) asymmetries. In terms of above said co-ordinates, for  $\ell$ -partial waves, the compound nucleus decay cross-section is given by

$$\sigma = \frac{\pi}{k^2} \sum_{l=0}^{l_{max}} (2l+1) P_0 P; \quad k = \sqrt{\frac{2\mu E_{c.m.}}{\hbar^2}} \quad (1)$$

Where,  $\mu = [A_1 - A_2 / (A_1 + A_2)]m$ , is the reduced mass, with  $m$  as the nucleon mass and  $l_{max}$  is the maximum angular momentum. Where  $P$  is the barrier penetration probability and  $P_0$  is the preformation probability at a fixed  $R$  on the decay path. The  $P_0$  are evaluated by solving stationary Schrödinger wave equation and  $P$  calculated as the WKB tunneling probability. The structure information in

\*Electronic address: birbikramsingh@sggswu.edu.in

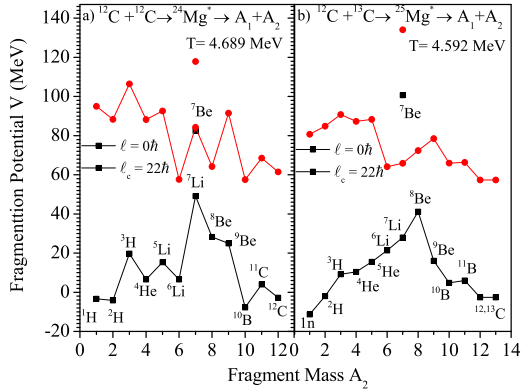


FIG. 1: The fragmentation potential as a function of fragment mass  $A_2$ , for the decay of CN (a)  $^{24}\text{Mg}^*$  and (b)  $^{25}\text{Mg}^*$ , for the spherical considerations of the nuclei.

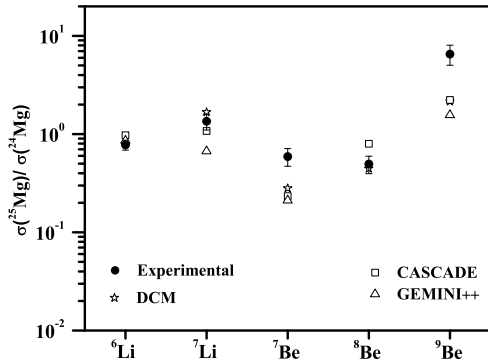


FIG. 2: The ratio of cross sections of the fragments in  $^{13}\text{C} + ^{12}\text{C}$  and  $^{12}\text{C} + ^{12}\text{C}$  reactions.

$P_0$  enters through the fragmentation potential  $V(\eta, R)$  as shown in Fig. 1.

## Calculations and Discussions

Fig. 1 shows the fragmentation potential as a function of fragment mass  $A_2$  for the decay of CN  $^{24}\text{Mg}^*$  (Fig. 1(a)) and  $^{25}\text{Mg}^*$  (Fig. 1(b)), for the spherical considerations of the nuclei. The minimized fragments  $^{6,7}\text{Li}$  and  $^{7,8,9}\text{Be}$  have strong competition from the neighbouring fragments. Moreover, we see that  $^7\text{Li}$  is strongly favoured in comparison to  $^7\text{Be}$  fragment, which is quite evident from Fig. 1 (separate dots are mentioned here on potential energy surface plot, for  $^7\text{Be}$  fragment).

Fig. 2 presents the ratio of total cross sections of the fragments  $^{6,7}\text{Li}$  and  $^{7,8,9}\text{Be}$  in  $^{13}\text{C} + ^{12}\text{C}$  and  $^{12}\text{C} + ^{12}\text{C}$  reactions. In

this plot, solid circles represent the experimental data whereas open stars and open squares, triangles represent the DCM calculations and statistical model calculations, respectively. For  $^{6,7}\text{Li}$  fragments, the complementary binary reaction products in the two reactions are  $^{19,18}\text{F}$  and  $^{18,17}\text{F}$ , respectively. The DCM calculated fragmentation of  $^{24,25}\text{Mg}^*$  into isotopes of Li and F is in very good agreement with the experimental data. However, the complementary fragments for  $^7\text{Be}$  are  $(^{17,18}\text{O})$ , among which  $^{18}\text{O}$  have well established cluster structure.

As observed experimentally [6], there is enhancement in the measured yield than statistical model calculations, which is a clear signature of the dominant role played by cluster structure. Here, DCM calculated result is in little better comparison due to inclusion of structure effects in the calculations. For the emission of  $^8\text{Be}$  the complementary decay channel  $^{16}\text{O}$  is well known  $\alpha$  cluster nucleus which boost up the yield of these exit channels. As a result,  $^8\text{Be}$  experimental yield ratio will be lower than the calculated yield and it will be just opposite for  $^9\text{Be}$ . We expect to improve the results further with the inclusion of deformation effects in the calculations. Work is in progress.

## References

- [1] A. Szanto de Toledo *et al*, Phys. Rev. Lett. **62**, 1255 (1989), M. M. Coimbra *et al*, Nucl. Phys. A **535**, 161 (1991).
- [2] BirBikram Singh, *et al.*, Proc. DAE Symp. on Nucl. Phys. **56**, 474 (2011); **57**, 550 (2012); **58**, 382 (2013); **59**, 346 (2014); EPJ Web of Conf. **86**, 00048 (2015); Conf. Proc. Jour. of Phys. **6**, 030001 (2015).
- [3] BirBikram Singh, Proc. DAE Symp. on Nucl. Phys. **61**, 510 (2016).
- [4] M. Kaur, *et al.*, Phys. Rev. C **95**, 014611 (2017); Nucl. Phys. A **969**, 14 (2018).
- [5] R. K. Gupta *et al.*, PRC **71**, 014601 (2005); IJMPE **15**, 699 (2006); PRC **77**, 054613 (2008); PRC **92**, 024623 (2015); R. Kaur *et al.* PRC **98**, 064612 (2018).
- [6] S. Manna *et al.* Phys. Rev. C **94**, 051601(R)(2016).